

# MOTION FLOW ESTIMATION FROM IMAGE SEQUENCES WITH APPLICATIONS TO BIOLOGICAL GROWTH AND MOTILITY

Gang Dong, Tobias I. Baskin

Department of Biology

University of Massachusetts

Amherst, Massachusetts 01003 USA

Kannappan Palaniappan

Department of Computer Science

University of Missouri-Columbia

Columbia, Missouri 65211 USA

## ABSTRACT

In this paper, a new method for motion flow estimation that considers errors in all the derivative measurements is presented. Based on the total least squares (TLS) model, we accurately estimate the motion flow in the general noise case by combining noise model (in form of covariance matrix) with a parametric motion model. The proposed algorithm is tested on two different types of biological motion, a growing plant root and a gastrulating embryo, with sequences obtained microscopically. The local, instantaneous velocity field estimated by the algorithm reveals the behavior of the underlying cellular elements.

**Index Terms**— image motion analysis, velocity measurement, biological cells.

## 1. INTRODUCTION

Motion estimation is one of the fundamental problems in the image processing field. It is a process to extract a field of velocity measurement of patterns from an image sequence. This velocity field is often called the optical flow.

Numerous studies, empirical and theoretical, have been performed on the optical flow estimation and its information content (see e.g., [1] and references therein). Performance evaluations of some of the most popular algorithms can be found in [2], [3]. Many optical flow formulations assume brightness consistency, i.e., the image brightness  $g(\mathbf{x}(t), t)$  is supposed to be stationary with respect to the time variable  $t$  and change only due to motion. Thus we have  $\frac{dg}{dt} = g_x u + g_y v + g_t = 0$ , for some constant  $c$ , where  $\mathbf{x} = [x, y]^T$  denotes spatial coordinates. This assumption leads to the well-known *optical flow constraint* by taking the temporal derivative

$$\frac{dg}{dt} = g_x u + g_y v + g_t = 0, \quad (1)$$

where  $\nabla g = [g_x, g_y, g_t]^T$  is a vector representing the spatio-temporal derivatives, and  $\mathbf{v} = [u, v]^T$  is a vector representing the optical flow field to be estimated.

Because the single equation of (1) is not sufficient to uniquely solve the unknowns, a fact referred to as the

aperture problem, additional constraints are needed. One approach often used is to assume that the velocity flow  $\mathbf{v}$  is locally constant in each small spatial neighborhood  $\Omega$  [4]. The flow estimate can then be estimated by minimizing the following least squares (LS) cost function

$$J_{LS}(\mathbf{v}) = \sum_{\mathbf{x} \in \Omega} (g_x u + g_y v + g_t)^2, \quad (2)$$

which is referred to as the Lucas-Kanade method [4]. The cost function can be interpreted as a measure of discrepancy how much the signal within that region fluctuates in the direction given by  $\mathbf{v} = [u, v]^T$ .

The use of classical LS method to estimate the optical flow implicitly assumes that the spatial derivatives are error-free and the errors are confined to the temporal derivative measurements. However, this noise model assumption is inconsistent with the fact that the observed image generally contains noise and all the spatio-temporal derivative measurements are computed numerically, which leads us to use the *total least squares* (TLS) method [5] or *errors-in-variables* (EIV) method [6] as known.

In this paper, as an extension work of [1], we propose an optical flow estimation algorithm with the following characteristics: 1) the errors in the spatial derivative measurements are taken into account based on TLS framework; 2) instead of the constant velocity assumption in [1], we use more flexible parametric model to describe the motion of each neighborhood and use all the tensors in that region to compute the motion parameters; 3) we formulate the problem in a close-form cost function that can be efficiently solved by suitable approximation schemes.

This work is motivated by the need to measure movements of biological objects. The growth and development of organisms is one of the most fundamental problems in biology. Automated and accurate measurement of growth is needed to evaluate the underlying mechanism for the size and form changes of biological objects, and to provide a non-intrusive tool for the morphogenesis analysis. In our work, sequences of two types of biological object, the root of the model plant *Arabidopsis thaliana* and the embryo of the frog *Xenopus laevis*, are used to illustrate the proposed algorithm.

## 2. TLS MOTION ESTIMATION

The LS method in (2) admits analytic solutions. However, the underlying assumption of LS is not realistic in applications since it implicitly assumes that the two spatial derivatives  $g_x$  and  $g_y$  are obtained without error. In fact, the image sequences are contaminated by noise generally. Thus, the use of numerical differentiation methods to compute the derivatives makes that the errors maybe present in all of the computed spatio-temporal derivatives components. Therefore, when information about the derivative measurement noise is available, it is desirable that it be incorporated into the estimation process.

Let  $\Lambda$  be the covariance matrix of  $\nabla g$  characterizing the uncertainty of the gradient components. We assume that the measurement noise has zero mean and the same covariance matrix at all pixels. We further assume that  $x$ -,  $y$ - and  $t$ - components of the noise are independent. The covariance matrix thus takes the form

$$\Lambda = \begin{bmatrix} \sigma_x^2 & 0 & 0 \\ 0 & \sigma_y^2 & 0 \\ 0 & 0 & \sigma_t^2 \end{bmatrix}. \quad (3)$$

Note that we have  $\sigma_x^2 = \sigma_y^2$  due to the fact that same kernel is used to compute both spatial gradients.

Letting  $\mathbf{v} = [v_x, v_y, v_t]^T$  as a 3D flow vector in spatiotemporal space, the solution of TLS estimation can be obtained by minimizing

$$J_{TLS}(\mathbf{v}) = \sum_{\mathbf{x} \in \Omega} \frac{[(\nabla g(\mathbf{x}))^T \mathbf{v}]^2}{\mathbf{v}^T \Lambda \mathbf{v}} = \frac{\mathbf{v}^T \mathbf{T} \mathbf{v}}{\mathbf{v}^T \Lambda \mathbf{v}}, \quad (4)$$

where

$$\mathbf{T} = \sum_{\mathbf{x} \in \Omega} [\nabla g(\mathbf{x}) \nabla g(\mathbf{x})^T], \quad (5)$$

is often referred to as the *structure tensor* [7]. This method can be deemed as a spatiotemporal variant of Lucas-Kanade method.

Because the matrix  $\Lambda$  is non-singular, the minimizer of  $J_{TLS}(\mathbf{v})$ ,  $\mathbf{v}_{TLS}$ , is an eigenvector of  $\Lambda^{-1}\mathbf{T}$  corresponding to the smallest eigenvalue. In practice, the singular-value decomposition (SVD) of  $\Lambda^{-1}\mathbf{T}$  is carried out to determine  $\mathbf{v}_{TLS}$ . Normalizing the third component of  $\mathbf{v}$  to one yields optical flow  $u = v_x/v_t$  and  $v = v_y/v_t$  as the first two components of  $\mathbf{v}$ .

## 3. TLS MOTION ESTIMATION WITH AFFINE MOTION MODEL

In this work, we introduce a constraint for the motion field  $\mathbf{v}$  within each localized neighborhood by assuming that  $\mathbf{v}$  can be described by an affine motion model. Often used as a simplified version of the perspective projection motion model, the affine motion model can be expressed as

$$\begin{aligned} \mathbf{v} &= \begin{bmatrix} v_x \\ v_y \\ v_t \end{bmatrix} = \begin{bmatrix} x & y & 1 & 0 & 0 & 0 & 0 & 0 & 0 \\ 0 & 0 & 0 & x & y & 1 & 0 & 0 & 0 \\ 0 & 0 & 0 & 0 & 0 & 0 & x & y & 1 \end{bmatrix} \begin{bmatrix} p_0 \\ p_1 \\ p_2 \\ p_3 \\ p_4 \\ p_5 \\ p_6 \\ p_7 \\ p_8 \end{bmatrix} \\ &\equiv \mathbf{B}\vec{p}. \end{aligned} \quad (6)$$

Although affine model is generally unsuitable for accurately describing 3D motion over a significant area of an image, it has been shown to offer a good inter-frame motion model for small localized image regions [8].

Substituting (6) into (4) shows that affine parameters  $\vec{p}_{TLS}$  can be solved by finding the minimum of the cost function

$$\begin{aligned} J_{TLS}(\mathbf{v}(\vec{p})) &= \sum_{\mathbf{x} \in \Omega} \frac{\vec{p}^T \mathbf{B}(\mathbf{x})^T \nabla g(\mathbf{x}) \nabla g(\mathbf{x})^T \mathbf{B}(\mathbf{x}) \vec{p}}{\vec{p}^T \mathbf{B}(\mathbf{x})^T \Lambda \mathbf{B}(\mathbf{x}) \vec{p}} \\ &= \sum_{\mathbf{x} \in \Omega} \frac{\vec{p}^T \mathbf{S}(\mathbf{x}) \vec{p}}{\vec{p}^T \Lambda_{\vec{p}}(\mathbf{x}) \vec{p}}, \end{aligned} \quad (7)$$

where

$$\mathbf{S}(\mathbf{x}) = \mathbf{B}(\mathbf{x})^T \nabla g(\mathbf{x}) \nabla g(\mathbf{x})^T \mathbf{B}(\mathbf{x}), \quad (8)$$

and

$$\Lambda_{\vec{p}}(\mathbf{x}) = \mathbf{B}(\mathbf{x})^T \Lambda \mathbf{B}(\mathbf{x}), \quad (9)$$

The matrix  $\Lambda_{\vec{p}}(\mathbf{x})$  denotes the covariance matrix for the different affine parameters at pixel  $\mathbf{x}$ . Mathematically, it can be proved that  $\vec{p}_{TLS}$ ,  $J_{TLS}$ -based estimate of  $\vec{p}$ , is equivalent to the maximum likelihood estimate given Gaussian noise model with covariance  $\Lambda_{\vec{p}}$ .

A similar work is presented by Liu *et al.* [9], where the summation of  $\mathbf{S}$  within a local neighborhood is called *parametric structure tensor*. It is shown that the least squares estimation of motion parameters  $\vec{p}$  can be recovered by solving a generalized eigenvalue problem (see [9] for details).

Now we are interested in finding the minimum of the TLS cost function in (7). The cost function is a nonlinear equation and is infeasible to admit solutions in closed form. However, a tractable approximation can be derived by employing a suitable numerical scheme. A commonly adopted method to minimize a function involving fractional expressions is proposed by Sampson [10]. We apply Sampson's method to minimize  $J_{TLS}$ . Let

$$M_k = \sum_{\mathbf{x} \in \Omega} \frac{\mathbf{S}(\mathbf{x})}{\vec{p}_k^T \Lambda_{\vec{p}}(\mathbf{x}) \vec{p}_k}, \quad (10)$$

for a specific  $\vec{p}_k$ . We have

$$J_{TLS} = \vec{p}^T M_k \vec{p}. \quad (11)$$

Note that each function  $J_{TLS}$  is now in the quadratic form of  $\vec{p}$ . Assuming that  $\vec{p}_{TLS}$  lies close to  $\vec{p}_{LS}$ , the numerical Sampson's scheme is implemented as follows

1. Find LS estimation  $\vec{p}_{LS}$  and initialize  $\vec{p}_0 = \vec{p}_{LS}$ .
2. Given  $\vec{p}_{k-1}$ , calculate the matrix  $M_{k-1}$ .

3. Compute the eigenvector of  $M_{k-1}$  corresponding to the smallest (but non-negative) eigenvalue by SVD, and choose this eigenvector as  $\vec{p}_k$ .
4. Steps 2 and 3 are then repeated using the newly estimated  $\vec{p}_k$  until convergence is reached. The condition for convergence is that  $\vec{p}_k$  is sufficiently close to  $\vec{p}_{k-1}$ .

In our case the convergence remains fast, no more than 4-5 iterations being needed.

#### 4. APPLICATIONS AND EXPERIMENTAL RESULTS

Our method has been tested on the *Yosemite* synthetic test sequence where the ground truth velocity field is known and on two real biological sequences: *A. thaliana* root and the *X. laevis* embryo sequences. In this section, we describe these tests and provide the experimental results. There is currently no ground truth data for the real test sequences; however, these sequences themselves provide strong visual cues about the flow directions so that we can evaluate the correctness of the results.

**Evaluation with the synthetic test sequence.** The *Yosemite* sequence is of the observer ‘flying’ through a synthetically generated landscape of Yosemite mountain. This sequence is mostly well textured, except that the sky part is much less textured and loosely maintains its intensity profile. The evaluation is performed by computing the *angular error measure* suggested by Barron *et al.* [1]. This error measure is given by  $\cos^{-1}(\mathbf{v}_{\text{est}} \cdot \mathbf{v}_{\text{true}})$  where  $\mathbf{v}_{\text{est}}$  denotes the estimated flow and  $\mathbf{v}_{\text{true}}$  denotes the true flow.

For all the tests, we use a spatiotemporal Gaussian filter with a standard deviation of 1.5 pixels-frames to smooth the sequences before further processing. The spatial neighborhood  $\Omega$  is  $15 \times 15$  pixels, wherein a Gaussian weighting function with a standard deviation of 3.5 pixels is utilized. The weighting function is used to give more constraints to the pixels at the center of the neighborhood than those at the periphery. Additionally, we use (9) to calculate each covariance matrix  $\Lambda_{\vec{p}}$ .

The evaluation results for the *Yosemite* sequence are summarized in Fig. 1 and in Table 1. In Fig. 1, we present original frame, the estimated velocity magnitude, and velocity in the form of vector field. The numerical results for the sequences with and without sky region are tabulated in Table 1 where the average error, the standard deviation and the percentage of motion vectors whose angular error is less than certain thresholds are given. By comparing with previously published results [1], it shows that our method achieves excellent accuracy in terms of angular error.

**Application to *A. thaliana* root sequences.** The plant species *A. thaliana* has been selected as an experimental tool among biologists for intense study due to its favorable

genetics. The objective here is to identify the pattern of growth velocity distribution to understand the mechanism of cell elongation and its relation to division within the growing region of the root [11]. In this experiment, the root is imaged in a series of overlapping stacks, each of which includes nine frames captured in the root’s growth zone.

For the purpose of studying root elongation, the component of the velocity field parallel to the root midline is of interest. The root midlines are determined manually to improve precision. Fig. 2 shows a representative sample of a velocity profile measured from multiple stacks by the proposed algorithm. The trends in the spatial distribution of velocity can be observed clearly in Fig. 2.

**Application to *X. laevis* gastrulation sequence.** The third experiment is performed on the *Xenopus laevis* sequence to investigate the morphogenetic movements involved in gastrulation and neurulation of the frog embryo during embryogenesis [12]. The spatial and temporal patterns of cell motility are visually noticeable in the example images shown in Fig. 3(a) and (b). The estimated optical flow magnitude profile and optical flow as vector field are depicted in Figs. 3(c) and (d), respectively. The recovered flow fields from our approach agree well with visual observation.

#### 5. CONCLUSION AND FUTURE WORK

We present a motion flow estimation algorithm, with application to recovery of biological growth velocity in particular. By incorporating a comprehensive TLS model, our method takes into account the errors in all of the measurements. The estimation accuracy is further improved using an affine parametric motion model. The biological velocity profile is traditionally estimated by marking growing organ regions using markers such as ink dots or graphite particles, and tracking the markers over time. Although this type of approach is potentially limited by the invasiveness of marking and by the small number of marks that can be applied, it provides a way to obtain ground truth data for quantitative algorithm evaluation and algorithm comparison between different optical flow algorithms and in which our work will be extended further.

#### Acknowledgement

We thank Prof. Ray Keller at University of Virginia for the gastrulation sequence. This work has been supported by the NIH Award EB00573-01A1.

#### References:

- [1] K. Palaniappan, H. Jiang, and T. I. Baskin, “Non-rigid motion estimation using the robust tensor method,” in *Proc. CVPRW*, vol. 1, pp. 25, 2004.
- [2] J. L. Barron, D. J. Fleet, and S. Beauchemin, “Performance of optical flow techniques,” *Int. J. Comput. Vis.*, vol. 12, pp. 43-77, 1994.

- [3] B. Galvin, B. McCane, K. Novins, D. Mason, and S. Mills, "Recovering motion fields: An analysis of eight optical flow algorithms," in *Proc. British Machine Vision Conference*, Southampton, England, 1998.
- [4] B. Lucas and T. Kanade, "An iterative image registration technique with an application to stereo vision," in *Proc. Seventh International Joint Conference on Artificial Intelligence*, pp. 674-679, 1981.
- [5] S. Van Huffel and J. Vandewalle, *The Total Least Squares Problem*. SIAM, Philadelphia, 1991.
- [6] B. Matei and P. Meer, "A general method for errors-in-variables problems in computer vision," in *Proc. Computer Vision Pattern Recognition*, vol. 2, pp. 18-25, 2000.
- [7] B. Jähne, H. Hassecker, H. Spies, D. Schmundt, and U. Schurr, "Study of dynamical processes with tensor-based spatiotemporal image processing techniques," in *Proc. ECCV*, vol. 2, pp. 322-336, 1998.
- [8] J. Giaccone, "Experiments in Recovering Affine Optical Flow," School of Computer Science, Kingstone University, 1996.
- [9] H. Liu, R. Chellappa, and A. Rosenfeld, "Accurate dense optical flow estimation using adaptive structure tensors and a parametric model," *IEEE Trans. Image Processing*, vol. 12, pp. 1170-1180, 2003.
- [10] P. D. Sampson, "Fitting conics sections to 'very scattered' data: An iterative refinement of the Bookstein algorithm," *Computer Graphics and Image Processing*, vol. 18, pp. 97-108, 1982.
- [11] G. T. S. Beemster and T. I. Baskin, "Analysis of cell division and elongation underlying the developmental acceleration of root growth in *Arabidopsis thaliana*," *Plant Physiology*, vol. 116, pp. 1515-1526, 1998.
- [12] R. Keller, L. A. Davidson, and D. R. Shook, "How we are shaped: The biomechanics of gastrulation," *Differentiation*, vol. 71, pp. 171-205, 2003.

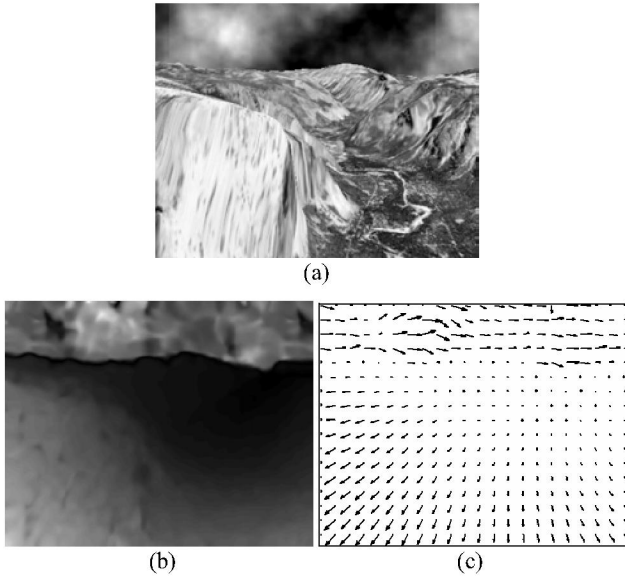


**Figure 1.** (a) Frame 8 from the Yosemite sequence with sky region, (b) estimated velocity magnitude profile, (c) estimated optical flow as vector field (subsampled).

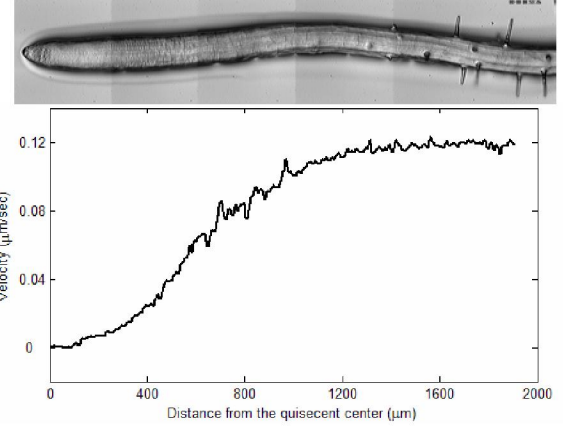


**Figure 2.** Velocity profile for *A. thaliana* root beneath a mosaic of the root, approximately to scale.

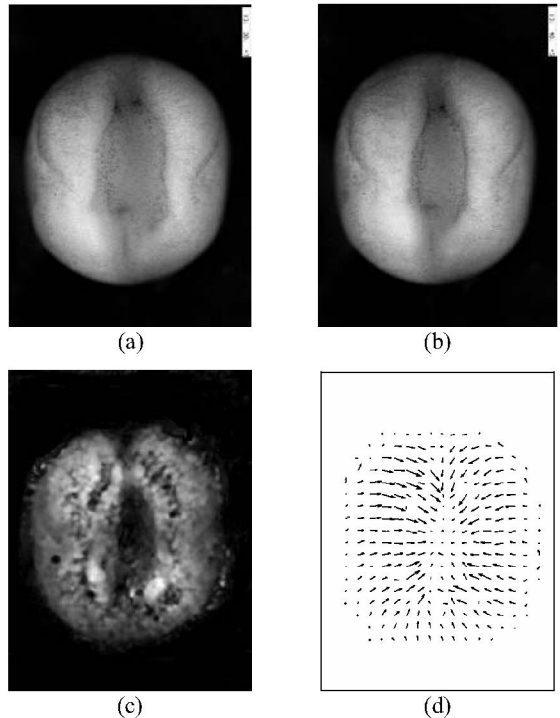


**Figure 3.** (a) Frame 1 from the *Xenopus laevis* sequence, (b) ditto, frame 9, (c) estimated optical flow magnitude profile, (d) estimated optical flow as vector field (subsampled).

**Table 1.** Flow estimation performance for Yosemite sequence.

	With sky region	Without sky region
Average angular error	5.26°	1.79°
Standard deviation of error	10.77°	3.65°
Estimated motion vectors with error less than	1°	32.3%
	2°	64.7%
	5°	89.2%
	10°	93.9%
		99.1%